

A comparison of rigid registration methods for prostate localization on CBCT and the dependence on rectum distension *

C Boydev^{1,2}, D Pasquier^{3,4}, F Derraz^{1,5}, L Peyrodie⁶, A Taleb-Ahmed¹ and JP Thiran^{2,7}

¹Laboratoire d'Automatique, de Mécanique et d'Informatique Industrielles et Humaines (LAMIH), Université de Valenciennes et du Hainaut-Cambrésis, France

²Signal Processing Laboratory (LTS5), École Polytechnique Fédérale de Lausanne, Switzerland

³Centre de Radiothérapie et d'Oncologie Galilée de Lille, France

⁴Département Universitaire de Radiothérapie, Centre Oscar Lambret, Lille, France

⁵Unité de Traitements de Signaux Biomédicaux (UTSB), Faculté Libre de Médecine, Lille, France

⁶Unité de Traitements de Signaux Biomédicaux (UTSB), Hautes Études d'Ingénieur, Lille, France

⁷Department of Radiology, University Hospital Center (CHUV) and University of Lausanne (UNIL), Switzerland

{christine.boydev, jp.thiran}@epfl.ch, d-pasquier@o-lambret.fr,

{foued.derraz,taleb}@univ-valenciennes.fr, Laurent.PEYRODIE@hei.fr

E-mail: christine.boydev@epfl.ch

Abstract. We evaluated automatic three-dimensional intensity-based rigid registration (RR) methods for prostate localization on CBCT scans and studied the impact of rectum distension on registration quality. 106 CBCT scans of 9 prostate patients were used. Each one was registered to the planning computed tomography (CT) scan using different methods: (a) global registration, (b) pelvis bony structure registration, (c) bony registration refined by a local prostate registration using the CT clinical target volume (CTV) expanded with 1, 3, 5, 8, 10, 12, 15 or 20-mm margin. Automatic CBCT contours were generated after propagation of the manual CT contours. To evaluate results, a radiation oncologist was asked to manually delineate the CTV on the CBCT scans (gold standard). The Dice similarity coefficients between propagated and manual CBCT contours were calculated.

1. Introduction

Daily image guidance, such as cone-beam computed tomography (CBCT) image-guided radiotherapy (IGRT) systems [1], has become a widely-used tool for patient repositioning in the treatment of prostate cancer. The prostate gland is known to be a moving and deformable gland under influence of rectal and bladder filling changes [2, 3, 4], which limits the effectiveness of skin marks in patient setup. Prostate localization on CBCT scans is challenging due to the relatively poor image quality [5, 6].

*This work was financially supported by ELEKTA SAS, Boulogne Billancourt, France.



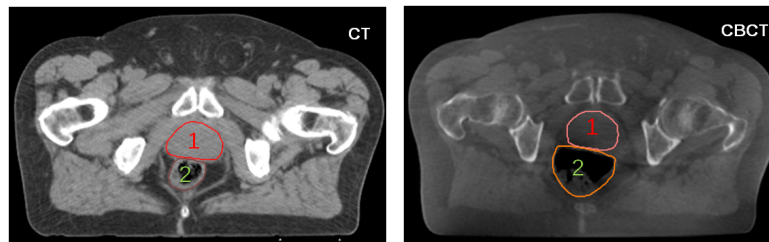


Fig. 1: Comparison of the image quality between (left) a CT scan and (right) a CBCT scan. The manual delineated contours of the prostate (number 1) and the rectum (number 2) are displayed. The display software used is VV (<http://vv.creatis.insa-lyon.fr/>).

This paper aims at evaluating different rigid registration (RR) methods for the purpose of prostate position verification. CBCT scans were rigidly registered to the planning CT scan and the manual delineated prostate contours were propagated from the CT scan to each CBCT scan to match the treatment anatomy. Deurloo *et al.* reported that the deformation of prostate during the course of radiotherapy is small compared to organ motion, and therefore in IGRT of prostate cancer, in first order, only setup error and organ motion need to be corrected for, whereas prostate deformation can be considered as a second-order effect [7]. RR accounts for first-order inter-fraction prostate motion. In our work, we tested different types of CT/CBCT RRs: global, bony, and local soft-tissue RRs. We also evaluated the impact of rectal distension on registration quality. Finally we drew up a couple of recommendations for clinical practice for the use of automatic RR for prostate localization on CBCT scans.

In this paper, we will use the terms clinical target volume (CTV) and planning target volume (PTV) as defined by the ICRU [8].

2. Material and methods

To automatically localize the prostate on the daily treatment CBCT scan, a CT/CBCT RR was performed and the resulting displacement was then applied to the contours manually drawn on the planning CT scan to generate the automatic CBCT contours. Three types of RR methods were tested:

- (a) global RR,
- (b) RR of the pelvis bony structures of CT and CBCT scans,
- (c) bony RR followed by local soft-tissue RR. The latter was conducted using a region of interest defined by the CT CTV expanded with a margin among 1, 3, 5, 8, 10, 12, 15 and 20 mm. The CTV represents the whole prostate gland and was manually delineated by the physician in the planning process, prior to treatment.

In the following, for the sake of simplicity, the combination of bony RR with local RR (method (c)) will be referred to as local RR.

2.1. Data collection

In total, 106 images of 9 prostate cancer patients were analyzed. All patients were instructed to follow a dietary protocol in order to have a full bladder and an empty air-free rectum at the time of the planning CT acquisition and during treatment. The planning CT data was acquired using a General Electrics Light Speed scanner. The treatment system was an ELEKTA Synergy linear accelerator (LINAC) equipped with CBCT imaging. During CT (CBCT) acquisition, the peak-voltage, X-ray tube current and exposure time were 120 kVp (120 kVp), 300 mA (40 mA or 64 mA) and 1000 ms (40 ms), respectively.

For clinical requirements, the prostate CTV was manually delineated on each planning CT scan by a radiation oncologist (this step is always required in clinical practice for treatment planning). For the purposes of this study, for validation, the same radiation oncologist manually delineated the CTV on each CBCT scan. The CT contours were used in the definition of the local registration mask. The CBCT contours were only used as ground truth in quantitative RR validation.

2.2. Registration Algorithm

Although the context is not strictly monomodal image registration, the relationship between the intensities on the CT image and those on the CBCT image is given by a linear equation. Hence the normalized-cross correlation metric was chosen as a suitable advanced cost function. The similarity between images was intensity-based, allowing registration to be fully automatic. Optimization was performed with the regular step gradient method. Transformations were rigid (six degrees of freedom, allowing translations and rotations). Linear interpolation was used in all our experiments. Three resolution levels were used.

For this study, all the data processing and visualization were performed on a Linux computer with distribution openSUSE 11.4 x86_64, with an Intel Dual Core i5-560M 2.66 GHz processor, 3MB L2 cache, 4 threads, and 8GB RAM.

For our implementation, the following open-source software, based on C++, was used:

- the Insight Toolkit ITK [9], freely available at www.itk.org,
- the ITK-based Command Line Image Toolkit cltk, freely available at <http://www.creatis.insa-lyon.fr/rio/cltk>.

The software versions used were ITK 3.20.1, CMake 2.8.3 and gcc 4.5.1.

2.3. Validation

To evaluate the RR results, we calculated the Dice similarity coefficient between the propagated CBCT contours and the manual CBCT contours (referred to as ground truth) [10]. Ideally, when the two volumes perfectly overlap, the Dice coefficient equals 1. A null Dice coefficient corresponds to two disjoint volumes.

2.4. Statistical analysis

Differences in the Dice results across the multiple RR methods were tested for significance using the inferential non-parametric Friedman statistical test (with α set to 0.05). The Wilcoxon-Nemenyi-McDonald-Thompson post-hoc test was conducted to decide which methods are significantly different from each other [11, page 295]. Software R was used [12].

2.5. Impact of rectal distension on local RR quality

The performance of RR is deteriorated when the size or the shape of an organ changes. When performing local RR on the prostate region of interest (ROI), the mask we use necessarily includes a portion of the rectum. However the rectum is highly prone to changes in size and shape due to its ever-changing filling (gaseous and solid contents). Our hypothesis we wish to validate is that unsuccessful local RRs are caused by the difference in rectal distension between the CT and the CBCT scans. In this study, we correlate unsuccessful local RRs to the difference in rectum filling between the images. For this purpose, on the CT scan, we calculated the average intensity, $\bar{I}_{CT,r}$, in the rectum portion included in the registration mask (or ROI). We used the manual segmentations to generate this region, $R_{partial_rectum}$, corresponding to the intersection of the ROI and the rectum volume on the CT scan. The rest of the rectum will not influence the registration process as only voxels that are inside the mask will be considered

for the calculation of the metric. We also calculated the average intensity, $\bar{I}_{CBCT,r}$, inside region $R_{partial_rectum}$ on the CBCT scan after rigidly aligning the bony structures of the CBCT and the CT scans. Because the overall range of intensities on a reconstructed CBCT scan can be shifted, we calculated $\bar{I}_{CBCT,p}$ that represents the CBCT average intensity inside the region corresponding to the CT manual prostate segmentation after rigidly aligning the bony structures of the CBCT and the CT scans, and we subtracted from the $\bar{I}_{CBCT,r}$. We used the following variable to quantify rectum filling variation:

$$F = |(\bar{I}_{CBCT,r} - \bar{I}_{CBCT,p}) - (\bar{I}_{CT,r} - \bar{I}_{CT,p})| \quad (1)$$

The F number given by Equation 1 consistently reflects the rectum distension. On a scan, an air-free empty rectum and a prostate, being both soft tissue, have the same range of pixel intensities. The rectum volume increases if its filling increases, i.e. when gas and solid contents appear. Gas and solid contents in the rectum have lower intensities than those in an air-free empty rectum.

We plotted the cumulative number of failed registrations, arranging the 106 CBCT scans in order of increasing F number. A registration was assessed as not successful if the Dice coefficient after registration was found to be lower than 95% of the Dice coefficient without registration.

3. Results

3.1. Statistical analysis

The statistical analysis showed that there was a highly significant difference between the following RR methods: (c)5mm vs (a) ($p = 2.0 \cdot 10^{-5}$), (c)5mm vs (b) ($p = 6.6 \cdot 10^{-8}$), (c)5mm vs (c)1mm ($p = 1.1 \cdot 10^{-6}$), (c)8mm vs (a) ($p = 2.0 \cdot 10^{-4}$), (c)8mm vs (b) ($p = 4.0 \cdot 10^{-7}$), (c)8mm vs (c)1mm ($p = 2.8 \cdot 10^{-5}$), and (c)10mm vs (b) ($p = 6.1 \cdot 10^{-3}$). All RR methods were found to yield Dice results significantly different from those obtained without registration. Statistically, RR gave the best agreement between the manual and the propagated contours when performed locally on soft tissue, with 5-mm or 8-mm CTV expansion. Table 1 shows the Dice medians, standard deviations (SD) and the number of failed registrations for each RR method. The Dice median without registration was found to be 0.742. The highest Dice medians were obtained with local RR with 5-mm and 8-mm margins. Conversely, bony RR appeared to be more robust than local RR methods as it counted the lowest number of failed registrations (5 cases over 106). When local RR with small margins failed, it could be caused by the lack of contrast and/or the frequently observed presence of (moving or not) gas pockets situated in the rectum and contiguous with the prostate membrane. We examined the few cases where bony RR failed, and it turned out that the Dice coefficients were all between 90% and 95% of the Dice coefficients without registration. We chose to focus, in the following, on the local RR with 8-mm margin as it produced the second best median after local RR with 5-mm margin and the second lowest number of failed registrations after bony RR.

| RR method | Global | Bony | Local | | | | | | | |
|----------------------|--------|-------|-------|-------|-------|-------|-------|-------|-------|-------|
| | | | 1 mm | 3 mm | 5 mm | 8 mm | 10 mm | 12 mm | 15 mm | 20 mm |
| Dice median | 0.786 | 0.785 | 0.787 | 0.806 | 0.823 | 0.819 | 0.806 | 0.796 | 0.799 | 0.796 |
| Dice SD | 0.071 | 0.066 | 0.097 | 0.140 | 0.088 | 0.075 | 0.084 | 0.064 | 0.076 | 0.068 |
| Failed registrations | 5 | 5 | 22 | 20 | 11 | 7 | 9 | 11 | 12 | 7 |

Table 1: Registration results. The median and the standard deviation (SD) of the Dice coefficients without registration were 0.742 and 0.109, respectively.

3.2. Impact of rectal distension on local RR quality

We investigated in which cases local RR with 8-mm margin failed. Figure 2 illustrates the impact of the variation of rectal filling between the images to be registered on the quality of local RR with 8-mm margin. We observed with our database that if the F factor as defined in Eq. 1 is lower than or equal to 112.6, registrations were all successful. All failed registrations appeared for values of F higher than 147.6. The range of F values obtained was from 0.2 to 406.6.

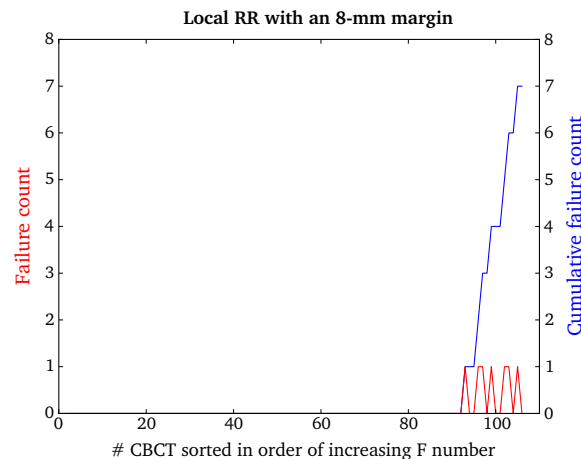


Fig. 2: Plot of (blue) the cumulative number of failed registrations and (red) its derivative, i.e. the failure frequency, obtained with local RR with 8-mm margin, against the CBCT scans arranged in order of increasing F number.

4. Discussion

Local RR with 8-mm margin was able to improve upon the Dice results obtained with bony RR as long as the rectal distension, that is the difference in the rectum anatomy between the planning CT scan and the treatment CBCT scan, is limited. For low values of F , results exceeded global RR or bony RR results, the latter being the current clinical standard for prostate repositioning. Smitsmans *et al.* found that 5-mm was the optimum margin for prostate CT/CT local RR [13]. In our study, we showed that indeed this method yielded the highest Dice median but it counted 11 failed registrations over 106, against only 7 failed registrations for local RR with 8-mm margin. Local RR with 8-mm has also a smaller SD than and a Dice median very close to those obtained with the 5-mm margin. That is why we preconize to use an 8-mm margin. In a later study, Smitsmans *et al.* also reported that local CT/CBCT RRs with 5-mm margin mainly failed because of streaks in the CBCT scans caused by moving gas pockets in the rectum during CBCT acquisition [14]. They implemented some improvements to their local RR algorithm, including the removal of the gray values of the pubic bone from the ROI. In our study, we could not find any correlation between the F factor defined in Eq. 1 and registration failures for local RR with margins lower than or including 5 mm. This is consistent with the fact that the lower the margin, the smaller the rectum portion included in the mask, and so the smaller the influence of the rectum portion on the registration process. Our assumption is that for margins lower than or including 5 mm, registration is not influenced by rectum distension.

Geometrical deviations occurring during treatment lead to target underdosage. To account for these geometrical deviations such as target volume delineation, organ motion and setup errors, a margin between the CTV and the PTV must be added. Van Herk *et al.* derived a margin recipe for prostate cancer radiotherapy, separating geometrical deviations into treatment execution

(random) and treatment preparation (systematic) variations [15]. An accurate daily verification and correction protocol of the patient setup before each treatment session should allow reducing treatment margins, after evaluating on clinical data the SD of random and systematic variations due to organ motion and residual setup errors after setup correction. Currently, CBCT-based daily verification and correction are widely performed using a bony RR in order to reduce the setup error. Furthermore a bony RR refined by a local RR with an 8-mm margin around the CTV as described in this paper should also reduce inter-fraction organ motion without the use of implanted fiducials markers.

5. Conclusions

With this study, we aim to provide guidance for good practice in the use of CBCT scans for prostate position verification and correction using RR. We recommend to start from the current clinical standard for prostate repositioning, that is, a RR on the pelvis bony structure. The next step is to determine whether local RR with 8-mm margin can be performed on top of the bony RR to improve upon registration quality. To do so, the user should evaluate the difference in rectum anatomy between the planning CT scan and the treatment CBCT scan. We propose, in this paper, a way to conduct such an evaluation, easily applicable in clinical practice, which uses the manual CT contours only and requires calculations of mean intensities in the prostate and in the portion of the rectum that is included in the registration mask. If the difference in rectum anatomy is limited, local RR performed on the CTV extended by an 8-mm margin will improve registration quality and prostate targeting. If not, the local RR may deteriorate registration quality and hence should not be applied. We highly recommend that the user should always visually assess the final registration quality, particularly when local RR is applied.

6. Conflict of interest statement

This work was financially supported by Elekta SAS, Boulogne-Billancourt, France.

References

- [1] Jaffray D A, Siewerdsen J H, Wong J W and Martinez A A 2002 *International Journal of Radiation Oncology*Biophysics* **53** 1337 – 1349 ISSN 0360-3016 1
- [2] Schild S, Casale H, Bellefontaine L *et al.* 1993 *Medical dosimetry: official journal of the American Association of Medical Dosimetrists* **18** 13 1
- [3] Roeske J C, Forman J D, Mesina C F, He T, Pelizzari C A, Fontenla E, Vijayakumar S and Chen G T 1995 *Int J Radiat Oncol Biol Phys* **33** 1321–1329 1
- [4] de Crevoisier R, Tucker S L, Dong L, Mohan R, Cheung R, Cox J D and Kuban D A 2005 *International Journal of Radiation Oncology*Biophysics* **62** 965 – 973 ISSN 0360-3016 1
- [5] Siewerdsen J H and Jaffray D A 2001 *Med Phys* **28** 220–231 1
- [6] Smitsmans M H P, Pos F J, de Bois J, Heemsbergen W D, Sonke J J, Lebesque J V and van Herk M 2008 *Int J Radiat Oncol Biol Phys* **71** 1279–1286 1
- [7] Deurloo K E, Steenbakkers R J, Zijp L J, de Bois J A, Nowak P J, Rasch C R and van Herk M 2005 *International Journal of Radiation Oncology*Biophysics* **61** 228 – 238 ISSN 0360-3016 1
- [8] Reviewer D J 1994 *Medical Physics* **21** 833–834 1
- [9] Ibanez L, Schroeder W, Ng L and Cates J 2005 *The ITK Software Guide* Kitware, Inc. ISBN 1-930934-15-7 <http://www.itk.org/ItkSoftwareGuide.pdf> 2nd ed 2.2
- [10] Dice L R 1945 *Ecology* **26** 297–302 2.3
- [11] Hollander M and Wolfe D A 1999 *Nonparametric statistical methods* (Wiley-Interscience) 2.4
- [12] R Core Team 2012 *R: A Language and Environment for Statistical Computing* R Foundation for Statistical Computing Vienna, Austria ISBN 3-900051-07-0 2.4
- [13] Smitsmans M H, Wolthaus J W, Artignan X, de Bois J, Jaffray D A, Lebesque J V and van Herk M 2004 *International Journal of Radiation Oncology*Biophysics* **60** 623–635 4
- [14] Smitsmans M H P, de Bois J, Sonke J J, Betgen A, Zijp L J, Jaffray D A, Lebesque J V and van Herk M 2005 *Int J Radiat Oncol Biol Phys* **63** 975–984 4
- [15] van Herk M, Remeijer P, Rasch C and Lebesque J V 2000 *International Journal of Radiation Oncology*Biophysics* **47** 1121 – 1135 ISSN 0360-3016 4